Renewable Energy 252 (2025) 123528

Contents lists available at ScienceDirect

Renewable Energy

journal homepage: www.elsevier.com/locate/renene

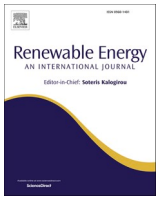

Evaluating the influence of different agrivoltaic topologies on PV energy, crop yields and land productivity in a temperate climate

Shu-Ngwa Asa'a [a,b,c,*], Silvia Ma Lu [d], Ismail Kaaya [a,b,c], Olivier Dupon [a,b,c], Richard de Jong [a,b,c], Arvid van der Heide [a,b,c], Sara Bouguerra [a,b,c], Hariharsudan Sivaramakrishnan Radhakrishnan [a,b,c], Jef Poortmans [a,c,e,f], Pietro Elia Campana [d], Michael Daenen [a,b,c]

[a] Hasselt University imo-imomec, Martelarenlaan 42, 3500, Hasselt, Belgium
[b] Imec, imo-imomec, Thor Park 8320, Genk, 3600, Belgium
[c] EnergyVille, imo-imomec, Thor Park 8320, Genk, 3600, Belgium
[d] Mälardalen University, Department of Sustainable Energy Systems, Box 883, 72123, Västerås, Sweden
[e] KU Leuven, Department of Electrical Engineering, Kasteelpark Arenberg 10, 3001, Leuven, Belgium
[f] Imec, Kapeldreef 75, 3001, Leuven, Belgium

ARTICLE INFO

Keywords:
Agrivoltaics
Sensitivity analyses
Energy yield
Crop irradiation
Crop yield
Land equivalent ratio

ABSTRACT

Agrivoltaics (AV) is a key technology to meet some of the sustainable development goals. In AV systems, light is the main limiting resource for crop growth. Hence, standard density photovoltaic (PV) designs could be detrimental to crop yields. The goal of this research was to assess the impact of new AV topologies on the land productivity. A solar irradiance and energy yield modelling framework was coupled with a crop model to assess the performance of south (S)-tilted, east-west (EW) vertical, and EW wing bifacial AV systems. For each AV system, continuous straight-line (standard), checkerboard, and dash-line PV arrangements were modelled, and the PV energy, sugar beet and winter wheat yields, and the land productivity assessed. Findings showed that crop yields were enhanced under lower PV densities, with up to 31% increase in winter wheat yields under EW wing checkerboard and dash-line designs compared to the standard layout. Specific energy was enhanced for the half PV densities by 2.5%, 4.2% and 2.3% for the S-tilted, EW vertical and EW wing respectively compared to the standard design. Specific energy yield of the S-tilted system was 25% higher than the EW vertical and 19.3% higher than the EW wing. Highest land equivalent ratio (LER) of 1.2 was obtained for sugar beets under S-tilted standard design. The LER was enhanced for all AV topologies, justifying their implementation and the potential of agrivoltaics to meeet the global energy and food demands.

1. Introduction

The continuous installation of renewable energy conversion technologies is a key step to mitigate climate change and meet the global energy demands. At the European level, renewable energies could help achieve the European Union's 2050 targets of climate neutrality [1]. Solar photovoltaics (PV) is a key technology to drive forward this energy transition and reduce the dependence on fossil fuels. The global cumulative installed PV capacity exceeded 2.2 TW_p at the end of 2024 [2], with the largest contribution from utility scale PV plants. This results in an extensive use of large areas of land, often competing with agriculture for the limited land resources. This is critical as food security is threatened by the impacts of climate change and an ever-increasing global population which is expected to reach 9.7 billion in 2050 [3]. Furthermore, at the European level, landscape fragmentation is a challenge to sustainable agriculture [4], and hinders the implementation of utility scale PV systems. Agrivoltaics (AV) is a suitable solution to alleviate this land use competition between PV and agriculture, by enabling the co-location of PV panels and crops on the same land for the simultaneous production of energy and food. Studies on different AV systems including the suitability of different PV technologies and crop performance under different shading scenarios [5] and a review of AV research projects [6] have been previously presented. In addition, the global installed AV capacity exceeded 14 GW_p in 2021 [7].

In some European regions like Flanders (Belgium), with a relatively

* Corresponding author. Hasselt University imo-imomec, Martelarenlaan 42, 3500 Hasselt, Belgium
E-mail address: shu-ngwa.asaa@uhasselt.be (S.-N. Asa'a).

https://doi.org/10.1016/j.renene.2025.123528
Received 21 February 2025; Received in revised form 9 May 2025; Accepted 18 May 2025
Available online 20 May 2025

List of abbreviations including units and nomenclature

AV	Agrivoltaics
CO_2	Carbon dioxide
DM	Dry matter
EW	East-west
GW_p	Gigawatt peak
GMPV	Ground-mounted photovoltaics
ha	Hectare
K	Agrivoltaics system size scale factor
kWh	Kilowatt hour
kWh/ha/yr	Kilowatt hour per hectare per year
kWh/m^2	Kilowatt hour per square meter
kW_p	Kilowatt peak
LER	Land equivalent ratio
Mt/a	Million tonnes per annum
MWh/ha	Megawatt hour per hectare
MWh/yr	Megawatt hour per year
PAR	Photosynthetically active radiation
PV	Photovoltaic
PVGIS	Photovoltaic geographical information system
S	South
TMY	Typical meteorological year
t DM/ha	Tonnes of dry matter per hectare
t/ha	Ton per hectare
TW_p	Terawatt peak
UTC	Coordinated Universal Time

high population density (about 500 people/km^2) [8] and agricultural land which is strewn between residential, industrialization, forestry, and nature [9], it is challenging to find suitable land for utility-scale PV systems. The implementation of suitable AV designs could therefore lead to a more efficient management of the limited space by fitting in small local niches. Furthermore, some high value crops and fruit trees are being protected from sunburn and hail damage by nets and plastic covers [10] which could be replaced by the integrated structures of PV panels. There are also concerns that the implementation of AV in such regions with relatively limited solar irradiation will further inhibit crop irradiation and crop yields. Therefore, a detailed study of different AV configurations which could ensure sufficient crop irradiation and potentially enhance the crop growth and land productivity would aid in AV crop selection and provide huge benefits in such regions. In addition, solar contributed only 11.9% to the electricity generation mix of Belgium in 2024, which is still lower than gas-powered generation (17.6%) [11].

Even with a temperate European climate, climate change has however led to continuously higher temperatures in the last two decades, with a projected continual warming till 2100 [12]. The changing weather could be detrimental to crop growth and yields. AV systems could therefore protect crops from climate change and provide a suitable environment for crop cultivation. AV also aligns with the common agricultural policy (CAP) Strategic Plan [13] by providing sustainable agriculture, additional income for farmers, climate change adaptation, resilient and quality soils, and improved water use efficiency. AV offers synergistic benefits as the PV panels protect the crops from adverse weather conditions such as hail, sunburn, snow, and wind loads, while the PV panels experience lower operating temperatures thanks to better wind convective cooling (due to installation at high elevations) and from crop transpiration [14]. In addition, the panels can protect early flowers and fruits from late spring frost by reducing radiative cooling [15]. AV systems can also reduce the irrigation needs of farmlands [16] thanks to less water loss from the soil by evaporation and from the crops by transpiration. Other cost benefits include the sale of generated PV electricity from the AV system, which could supplement the income of farmers [17]. AV therefore brings benefits across the food-energy-water nexus.

Despite these benefits, the implementation of PV modules above crops inherently leads to shading which could reduce the crop yield or quality [18]. This shading could be reduced by optimizing the AV design parameters such as the PV row distance, elevation, tilt angle, orientation and the PV array arrangement. The latter is vital, as the main reason for optimizing the AV array design is to manage the light distribution, which is the limiting resource [19]. Therefore, by using different AV topologies and modifying the PV array density, the degree of shading on the crops can be modulated. Moreover, crops whose light requirements align with the light availability in each AV design can be selected to increase the crop yields.

Previous simulations on AV have mainly focused on standard PV configurations and their impact on the energy and crop light distribution. For example, simulations with East-West (EW) vertical and South (S)-tilted AV systems in Foulum (Denmark) showed that the vertical system created more uniform ground irradiation [20]. It was also reported that EW vertical bifacial systems offered better spatial crop light distribution compared to north-south monofacial AV systems, while both systems showed similar crop and energy yields when the PV density was half that of ground-mounted PV (GMPV) systems [21]. Simulations on two different PV layouts in South Korea reported that PV modules in landscape orientation created higher shading ratios and higher power generation while the portrait format increased crop irradiation [22]. Studies on the irradiance on a pear orchard canopy under an EW wing system in Bierbeek (Belgium) reported heterogeneous light distribution under checkerboard PV pattern [23]. The crop irradiance distribution and energy yields for south facing, EW vertical and EW wing AV systems have been previously simulated under the Boston (USA) climate [24]. It was reported that EW wing enhanced the homogeneity of the crop light distribution while S-tilted and EW vertical checkerboard PV patterns resulted in patchy shading. However, the impact of the different topologies on crop yields and the total land productivity was not assessed. To the best of the authors' knowledge, there is still a clear research gap in the combined impact of different AV configurations and PV arrangements on the crop light distribution, crop and PV energy yields and the total land productivity. Furthermore, standard PV installations or densities could lead to non-uniform and insufficient irradiation on crops, and a reduction in the crop yields and the land productivity. To address this research gap, in this study, an irradiance and energy yield modelling framework is coupled with a crop model to demonstrate how nine different AV topologies impact the total land productivity. Using winter wheat and sugar beet under a temperate climate as a case study, the PV energy yields, crop irradiance distribution, crop yields and the total land productivity for the different AV topologies are assessed and compared. Findings from the illustrated AV configurations are used to recommend suitable AV designs and crops for regions with a temperate climate. Optimization of AV topologies is very valuable in regions with limited solar irradiation, high population densities and fragmented landscapes, looking to transition to AV installations.

This paper is structured as follows: Section 1. provides the introduction and highlights the novelty of the research, Section 2. describes the modelling and simulation approach for the irradiance modelling and the energy and crop yields. Section 3. presents and discusses the results, focusing on trade-offs in AV system designs, crop irradiation, energy and crop yields and the total land productivity. Section 4. discusses the limitations of this study and areas for future research. Section 5. summarizes and concludes with the findings from this research.

2. Methodology

To precisely simulate the distribution of solar irradiation, energy yield, and shading effects of PV modules on crops, the modelling approach employed must be both robust and flexible enough to accommodate different AV topologies. In this work, imec's simulation framework, which is based on bifacial ray tracing was used [25,26]. Fig. 1 shows an extended schematic of the modelling approach and parameters. To demonstrate this methodology in a temperate climate, the location of Genk, Belgium (50.9662° N, 5.5022° E) was selected. The simulations are based on hourly weather data for a typical meteorological year (TMY) obtained from PVGIS [27]. The modelling process is divided into three stages: geometric, irradiance, and yield (energy and crop) modelling.

2.1. Geometric modelling: the scenarios

The simulated AV farms consisted of PV modules at given row distances (p), tilt angles (α) and elevations (e). In this work, three PV orientations were defined: S-tilted, EW vertical and EW wing as shown in Fig. 2. SketchUp Pro 2023 was used to create the 3D geometric models of the PV modules. A 60-cell bifacial module with aluminum frame was modelled and a "scene generator" tool was used to create the string of modules which was then extended to the PV array making up the AV system. The "scene generator" is a Python script which generates the geometries of the AV systems' components in a virtual environment based on pre-defined input parameters such as the tilt, elevation, row distances, azimuth and array length. To reduce the computational time, the support structures and hence their associated shading effects were not included in the modelling of the AV system. To investigate the impact of the PV density and different PV arrangements on the homogeneity of the crop irradiance distribution and crop yield, three PV patterns for each orientation were modelled: a continuous straight-line (standard layout), checkerboard, and dash-line. Fig. 3A–C shows the dash-line pattern in which adjacent PV modules in a row are spaced apart by the size of a PV module. Fig. 3D–F shows the checkerboard patterns. In both the dash-line and checkerboard patterns, the PV density is half of the straight-line pattern.

2.2. Irradiance modelling

Given the different AV farm configurations and the use of bifacial PV modules, the irradiance modelling approach should accurately predict the front and rear PV irradiance and the irradiation on the crops. In this work, ray tracing was used in the optical modelling. In applications where light interaction with material properties (e.g., emissivity, transmissivity, and reflectivity) must be considered, ray tracing is used [28]. Radiance employs backward ray tracing, wherein light rays are traced in the opposite direction to which they are projected, that is, from target to the source or emitter [29].

The layout of the PV modules, crops and ground were defined by assigning material properties to the different components. The PV arrays were then given tilt angles and orientations which were used in the optical process to convert the measured irradiances into the irradiance on the plane of PV array according to the Perez model [30]. To accurately identify the materials in Radiance, the materials were given pre-defined Radiance material properties such as plastic (RadPlastic), glass (RadGlass) and metal (RadMetal), which determine how light interacts with the geometric surfaces [29]. Radiance deals with a single band of red, green, and blue (RGB) colors, and these are used in the definition of the optical properties. The reflectance properties of the crops were defined by the measured reflectance spectra of the green leaves from a Dracaena plant as shown in Fig. 4. The reflectance showed a similar spectral shape of green plant leaves [31], with an average reflectance of 11% in the red (640–700 nm), 16% in the green (500–570 nm) and 8% in the blue (400–490 nm) spectra.

The solar cells were defined in Radiance using the RadPlastic category, which takes five parameters defined by RGB reflectance,

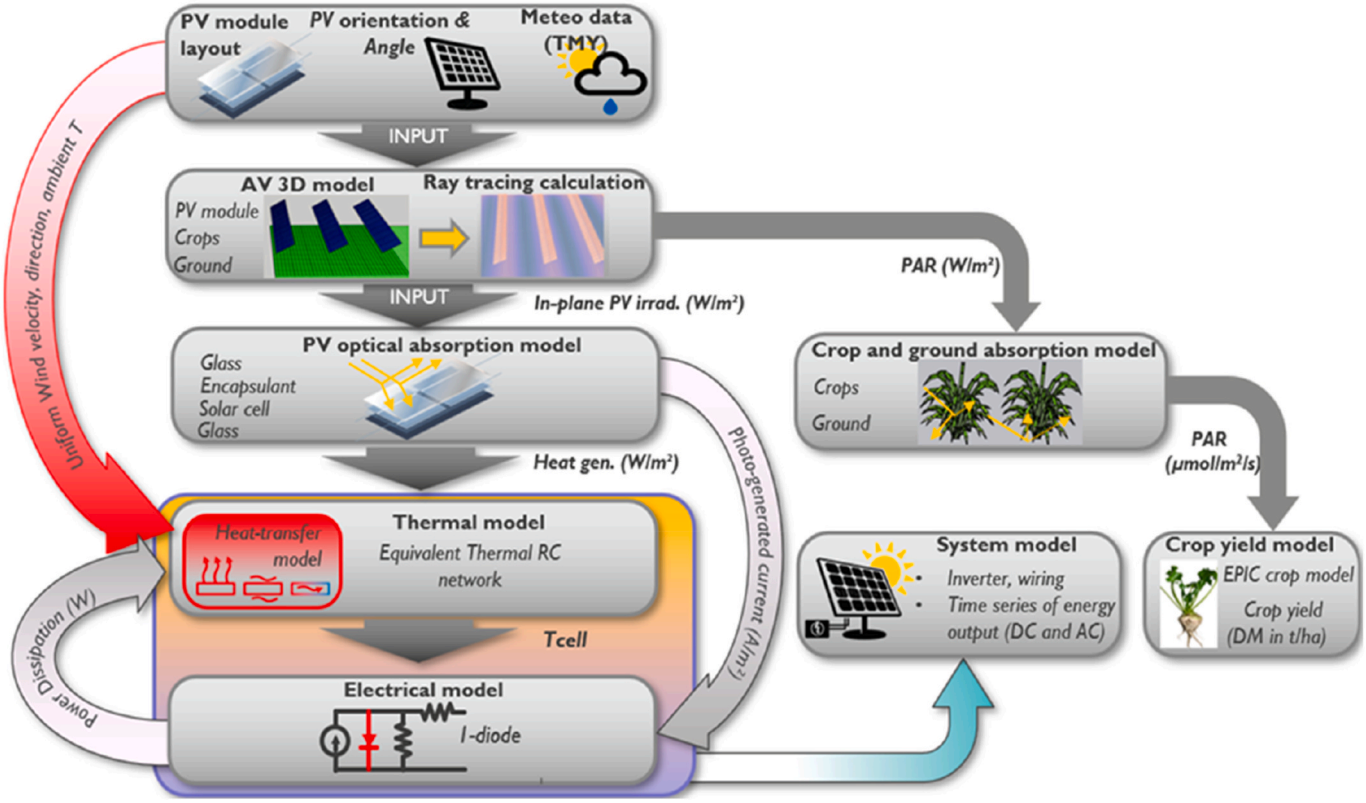

Fig. 1. Schematic of the AV modelling framework. Main outputs are the DC power output and the crop dry matter (DM) yield in tonnes per hectare (t/ha).

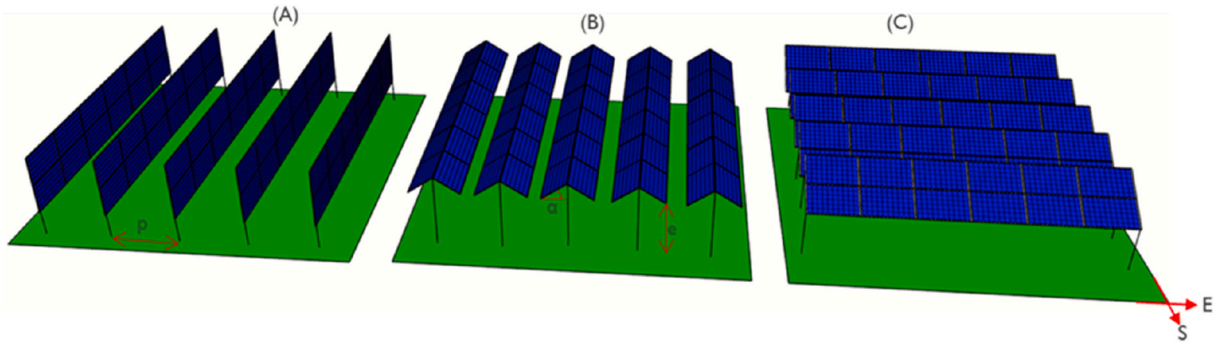

Fig. 2. Illustrations of the three bifacial AV systems studied in this work. (A) EW vertical (EW vert), (B) EW wing, and (C) S-tilted. Models were created with SketchUp Pro and show the PV modules in the straight-line pattern. Geometric models shown here for the same installed capacity.

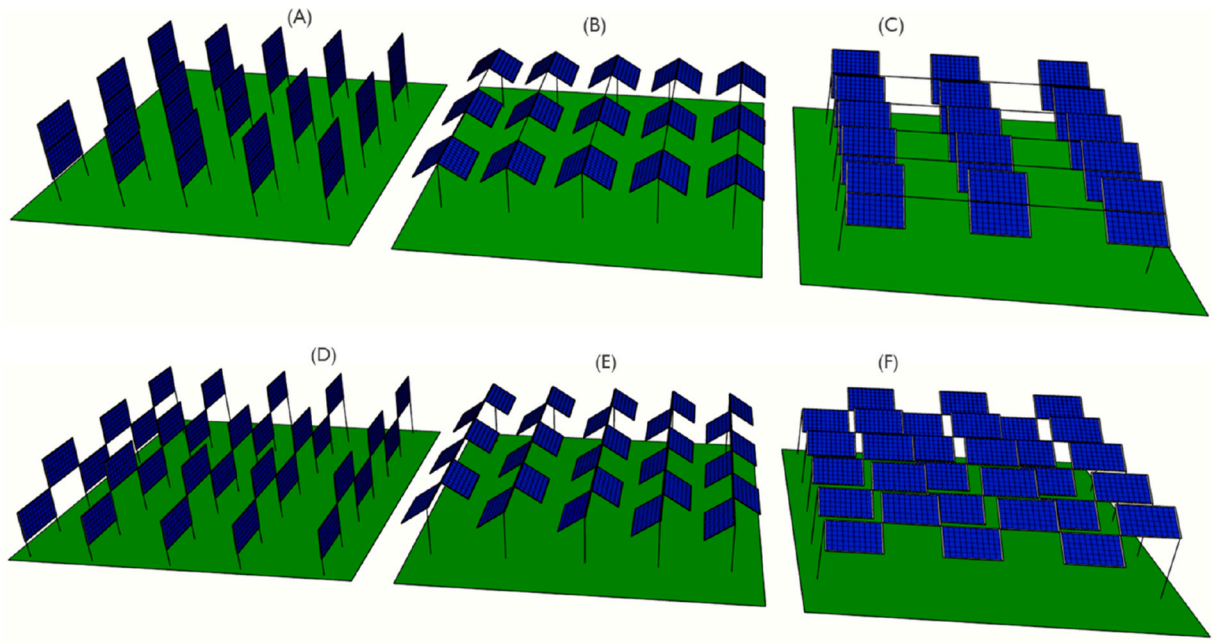

Fig. 3. Illustrations of the different AV arrangements. The dash-line patterns for the (A) EW vertical, (B) EW wing, (C) S-tilted and the checkerboard patterns for (D) EW vertical, (E) EW wing and (F) S-tilted AV systems.

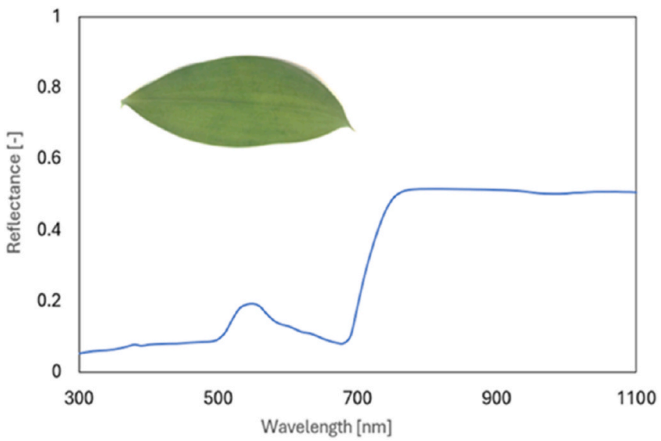

Fig. 4. Reflectance spectra of the green leaves of a Dracaena plant measured using a spectrophotometer. Measured RGB reflectance values are used as input for the crop Radiance parameters as shown in Table S1.

specularity, and roughness values [32]. The RGB parameters define the overall material color and represent the diffuse reflectance in these colors. The specularity describes the specular reflectance and refers to the gloss of the material, while the roughness defines the surface roughness. The soil and crop were also assigned the RadPlastic material category. However, the specularity and the surface roughness of the RadPlastic were neglected in order to faithfully represent the optical properties of the materials defined. Furthermore, to identify the front and rear PV module glasses in Radiance, the RadGlass category was used, and represents a material that refracts and transmits light. The RadGlass type is defined by a refractive index and transmission in the RGB at normal incidence. Finally, the PV module frame (usually made of aluminum) was defined using the RadMetal property which takes similar parameters as the plastic, except the fact that its highlights are altered by the material color. More details on the Radiance material properties have been described in Ref. [32]. The optical properties of the different materials and geometries in the AV system are shown in Table S1 in Supporting Information. The amount of light which reaches the rear of the PV module is strongly dependent on the albedo of the surface below. In this study, a broadband albedo of 0.22 was used for the ground.

2.3. Energy yield modelling

The main features and approach of the PV energy yield modelling have been previously described in Ref. [25]. A maximum power point tracking (MPPT) algorithm was added at the PV string level. This made it possible to assess the DC power output in real life conditions while accounting for temporal fluctuations and non-uniformities such as mismatch due to partial shading. To further mitigate mismatch losses due to shading, the cell strings in each module were modelled with bypass diodes as shown in Fig. 5.

The specifications of the PV module used in the simulation are shown in Table S2 in Supporting Information. The main output from the PV energy simulation was the instantaneous DC output power at the maximum power point. A power bifaciality factor of 80% was also used for the PV module. The power bifaciality factor used is close to the upper limit of that of PERC cells [33,34]. The effective PV module irradiation is represented in equation (1). Table S3 (Supporting Information) summarizes the system losses considered in the annual AC energy yield.

$$G_{eff} = G_{front} + \gamma^{*} G_{rear} \quad (1)$$

Where G_{eff} is the effective bifacial irradiance in W/m^2, and G_{front} and G_{rear} are the irradiances on the front and rear of the bifacial PV module respectively. γ is the bifaciality factor.

2.4. Crop model

The crop yield modelling approach used in this study is built upon the model presented in a previous agrivoltaic study [35], which itself is an adaptation of the Environmental Policy Integrated Climate (EPIC) model [36]. This model estimates the actual crop yield in tonnes of dry matter per hectare (t DM/ha) based on radiation use efficiency, daily intercepted photosynthetically active radiation (PAR), and additional relevant parameters (e.g., weather and the crop-specific factors). The model accounts for influences such as temperature stress, water stress, and nutrient availability to determine the daily crop growth (biomass) and leaf area index (LAI) development. Further details on the model have been described in Ref. [35].

In this study, the yields of sugar beet (*Beta vulgaris* L.*)* and winter wheat (*Triticum aestivum* L.), commonly grown arable crops in Belgium and Europe [37] were simulated under the different AV designs presented. Table S4 in Supporting Information shows the crop-specific input parameters for winter wheat and sugar beet, particularly under Belgian climatic conditions. The harvest index used in Ref. [38] was considered as the ratio of the grain biomass to the total above-ground biomass (shoot) for winter wheat and as the ratio of the root biomass to the total plant (shoot and root) for sugar beets. The weather file used was based on the TMY data from PVGIS [27] while the precipitation data was obtained from the Royal Meteorological Institute (RMI) of Belgium [39]. The daily PAR reaching the crops under the different AV designs was calculated using the output irradiance data from section 2.2, which is the average irradiance reaching the total crop area. The global irradiance on the crop canopy was converted to PAR based on the conversion factor of 45% [40]. Simulation results by the authors (data not shown) revealed that the PAR percentage in Belgium lies around this value.

2.5. Land equivalent ratio

The LER indicates the efficacy of the AV system compared to separate crop and PV energy production systems [41]. The LER is calculated according to equation (2).

$$LER = \frac{Y_{cr,AV}}{Y_{cr,ref}}(1 - LL) + \frac{Y_{e,AV}}{Y_{e,ref}} \quad (2)$$

Where $Y_{cr,AV}$ is the crop yield (t/ha) under the AV system, $Y_{cr,ref}$ is the crop yield in the unshaded reference system (t/ha), $Y_{e,AV}$ is the AV energy yield (MWh/ha) and $Y_{e,ref}$ is the energy yield from the reference or GMPV system (MWh/ha). LL is the land loss and is attributed to the crop, as it represents the percentage of land under the AV array not used for crop cultivation due to the presence of the support structures. A LL value of 10% was used as previously estimated in Ref. [41]. The reference GMPV system is a double-stacked monofacial S-tilted PV system with an elevation of 0.5 m, row-distance of 3 m and 35° south tilted.

2.6. Edge effects in AV systems

The ground irradiation distribution and energy yield in AV systems are influenced by edge effects. Given the higher elevations (particularly for overhead systems) and row distances in AV systems compared to GMPV, the edge effects are expected to be higher especially in locations or during periods with low solar elevations. Therefore, the size of the modelled AV farm should be large enough such that these boundary effects are minimized. This is because edge effects reduce the accuracy of scaling up and predicting crop and energy yields. A sensitivity analysis was carried out to identify the AV system size at which the edge effects are minimized by assessing the relative ground irradiation G_{rel} (irradiation in AV systems compared to an open field) as shown in equation (3).

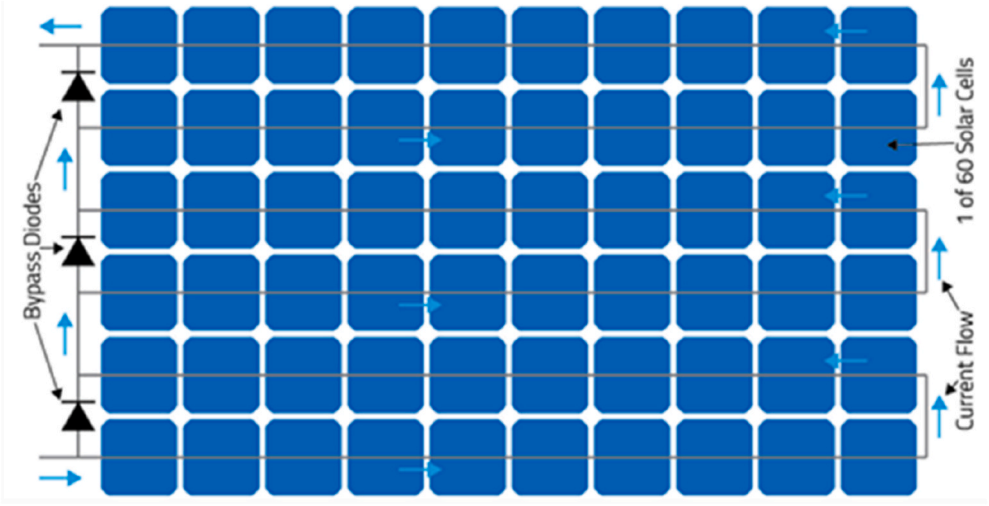

Fig. 5. Layout of the 60-cell bifacial PV module used in energy yield simulation.

$$G_{rel} = \frac{G_{AV}}{G_{open}} \quad (3)$$

Where G_{AV} is the average ground irradiation in the AV systems and G_{open} is that in an open (reference) field.

3. Results and discussions

This section presents and discusses the sensitivity studies on required system size for edge effect minimization and the impacts of design parameters such as the tilt angle and row distance on the PV energy yield and the relative crop irradiation. The crop irradiance distribution, specific energy yields, crop yields, and land productivity for the different topologies are also assessed.

3.1. Sensitivity analyses on AV system designs

3.1.1. System size and edge effects minimization

For a given S-tilted AV system of size K = 1 (9.92 m × 16.5 m) defined by the width and length of the farm respectively, the total AV system was extended in both length and width, and the G_{rel} assessed. To account for the seasonal variability in ground irradiation, four days were selected: a clear sky and a cloudy day in the summer (June) and a clear sky and cloudy day in winter (January). By increasing the system size with scale factors (K = 1,2,3 …), the G_{rel} gradually reduced and began saturating around K = 20 (198.4 m × 330 m) as seen in Fig. 6. Beyond this size, the reduction in the relative ground irradiation (impact of edge effects) was less than 0.2%. This can be considered the minimum total AV area for the given location to be simulated for which edge effects are minimized. The clear sky days (orange and yellow curves) had slightly steeper slopes as the ground irradiation saturated at a slower rate, compared to the cloudy days (blue and gray curves). This can be attributed to more diffuse light for cloudy days which increases the spatial and temporal distribution of light under the PV modules. Hence the uniformity of the ground irradiation increases and saturates faster under diffuse conditions.

The computational burden of simulating such AV system sizes is high, as ray tracing is a very computationally intensive method [42]. To reduce this, while faithfully minimizing the border effects, the central area of a relatively smaller AV system can be used instead. Hence, by considering the central AV sample of size K = 1 (9.92 m × 16.5 m) while extending the total ground area, a system size K = 4 (39.68 m × 66 m) was reached. Hence, by using this central AV farm area (0.016 ha) of the total ground (0.26 ha), the AV system studied is not influenced by the boundary effects. Fig. 7A shows the extension analysis of the total AV ground area for the sample AV field studied. Hence the AV field sample simulated (Fig. 7B) represents the center of an AV farm without edge effects. This area also represents the farm area used in the crop yield modelling. Furthermore, by positioning the PV modules at the center of the farm, the edge effects on the central PV array and central farm area are minimized.

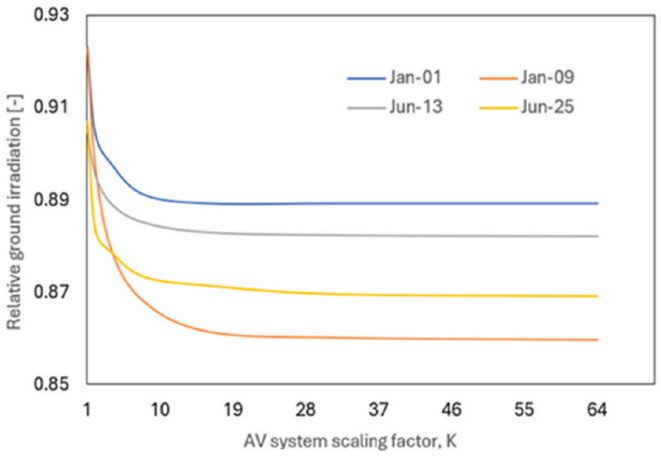

Fig. 6. Sensitivity analyses on the impact of AV ground size on the relative ground irradiation. System size K = 1 (9.92 m × 16.5 m) represents a given AV system size which is scaled in both length and width by various factors from 1 to 64. Results are shown for two clear sky days (Jan 9 and Jun 25) and two cloudy days (Jan 1 and Jun 13).

3.1.2. Design of EW vertical AV system

An analysis of the existing trade-offs between the energy yield and the relative crop irradiation for varied row distances is shown in Fig. 8. For PV modules installed 1 m above the ground, the crop irradiation increased with row distance, while the energy yield decreased. The reduction in energy yield was due to a lower installed PV capacity with increasing row distance. On the other hand, the specific PV energy yield is expected to increase with row distance due to reduced mutual PV row shading and increased ground reflected light reaching the PV panels. The increased row spacing also allows greater wind flow which could result in lower PV module temperatures and higher energy yields. Nevertheless, more land is needed for the same energy yield as the PV arrays are more spaced out and the balance of system costs (e.g., wiring costs, civil works) are higher [43]. The gain in crop irradiation with increasing row distance was due to reduced PV shading and increased light penetration. As the row distance increased from 2 m to 20 m, the crop irradiation increased by 95.1% while the energy yield reduced by 75%. This trade-off in the PV array design necessitates the effective design and use of the agricultural land. In this work a row distance of 10 m was used.

As the modules are double stacked in landscape (2 L), assessing the irradiance distribution on the top and bottom PV modules is vital in the electrical design and in predicting the energy yields and electrical wiring for the MPPT. Hence, the average yearly irradiance on the top and bottom PV modules was simulated as shown in Fig. 9. The irradiance on the top PV arrays was higher than the bottom for both the center and edge arrays. Hence, higher energy yields are expected for the top PV arrays. Similar results have been reported in Ref. [44]. The higher elevation of the top PV array also leads to better convective cooling and hence lower operating temperature which has a positive impact on the energy yields [45]. However, it was reported that the higher irradiance on the top PV array increases the module temperature and overrides the benefits of the convective cooling [44]. Moreover, for the farthest PV arrays on the east and west sides (not considered), the irradiance was much higher than the center arrays, due to the edge effects. Hence, the edge effects could increase the difficulty in directly scaling and accurately predicting the energy yield.

3.1.3. Design of S-tilted AV system

The relative crop irradiation and energy yield for varied row distances were also assessed for the S-tilted system as shown in Fig. 10A. Like the EW vertical system, a tradeoff exists in the energy yield and the relative crop irradiation. As the row distance increased from 3 m to 9 m, the energy yield reduced by 67% while the crop irradiation increased by 129.3%. Further tradeoffs for varied PV module tilt angles are shown in Fig. 10B. Similarly, as the energy yield increased, the relative crop irradiation reduced and vice versa. For the chosen location of Genk, the maximum energy yield was obtained at a tilt angle of 35°. In this work a row distance of 6 m and an elevation of 5 m were used.

3.1.4. Design of EW wing AV system

For the EW wing system, similar tradeoffs between the energy yield and the crop irradiation exist (Fig. 11) as for the S-tilted system. As the row distance increased from 3 m to 9 m, the energy yield decreased by 70.3% while the relative crop irradiation increased by 107.5%. The gain in crop irradiation with increasing row distance was lower for the EW wing system compared to the S-tilted. This implies the S-tilted system

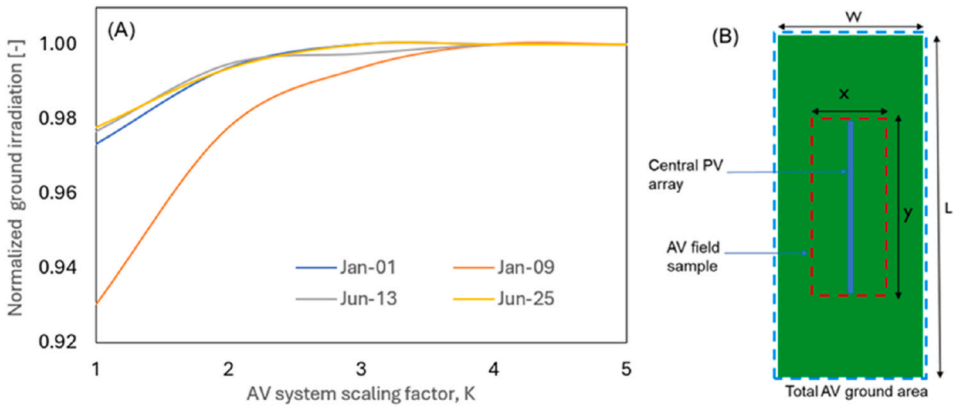

Fig. 7. (A) Normalized AV ground irradiation for the ground area extension sensitivity. (B) Top view of the total AV ground area, K = 4 (39.68 × 66 m^2) and the AV field sample (9.92 × 16.5 m^2) without edge effects used in the modelling and irradiance analysis.

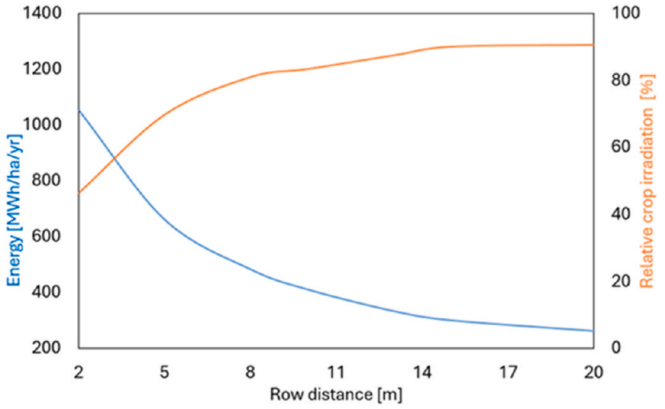

Fig. 8. Sensitivity analysis of annual relative crop irradiation and energy yield for varying row distances for EW vertical system.

offered higher light penetration to the crops compared to the EW wing for increasing row distances. Similar tradeoffs in energy yield and crop irradiation were observed for varied tilt angles, with a maximum energy yield around 6° tilt. However, for this work, a tilt angle of 12° was used as the soiling rate is higher at very low tilt angles [46]. Furthermore, the difference in energy yield between 6° and 12° tilt angles was only 0.8%.

In addition, a row distance of 5 m and an elevation of 5 m were used in this study. Table S5 in Supporting Information summarizes the different design parameters for the S-tiled, EW vertical and EW wing systems used in this study.

While the impacts of the PV row distance and tilt angle on the energy yields and crop irradiation are well defined, the row distance is also influenced by the tilt angle. Higher tilt angles could lead to excessive shading of adjacent PV rows due to extended shadows cast by the PV arrays especially during low solar elevations. Hence, higher row distances will be required to mitigate this shading. However, an increased row distance is accompanied by a reduction in the installed PV capacity per ha and potentially higher wiring costs and resistive cable losses. Given these clear tradeoffs between crop irradiation and energy yield and the interdependent relationship between the tilt angle and row distance, design considerations for AV systems should be different from GMPV systems and must consider the light requirements of the crops while minimizing mutual PV shading. The AV system design should utilize the agricultural land sustainably by prioritizing the crop needs to avoid extensive exploitation of farmland for energy yield. In cases where energy yield is prioritized, potential trade-offs can be minimized by selecting shade tolerant crops such that crop yields and the land productivity can be maximized.

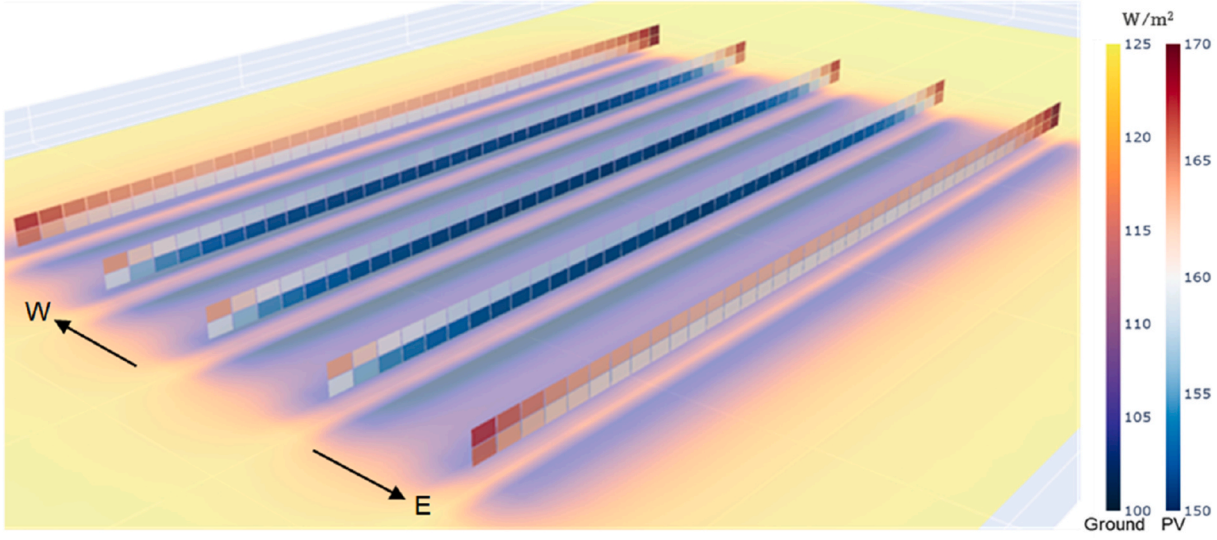

Fig. 9. Yearly average irradiance on the ground and the top and bottom PV modules of the EW vertical system at 10 m row distance.

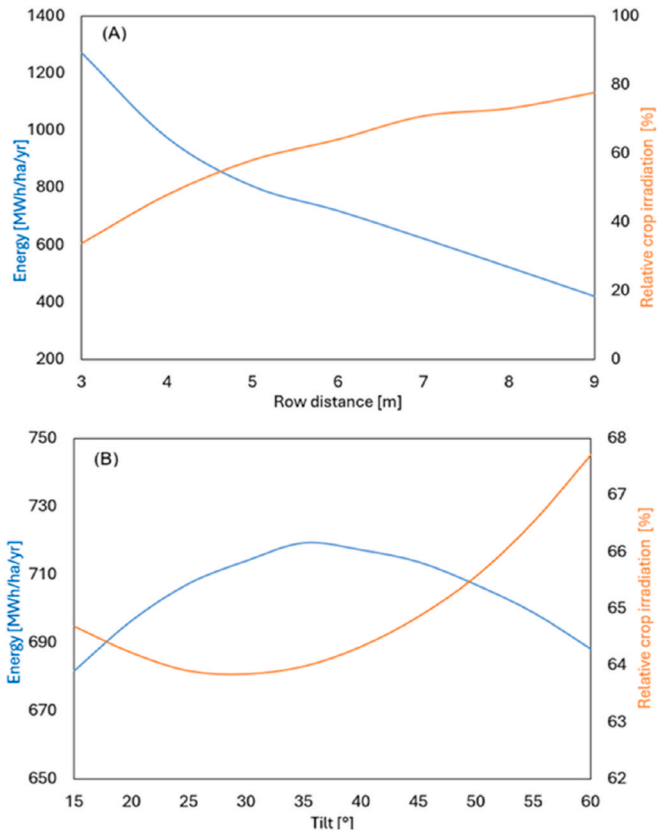

Fig. 10. Sensitivity study of the annual relative crop irradiation and energy yield for the S-tilted system for (A) varied row distances at 35° tilt, and (B) varied tilt angles at 6 m row distance.

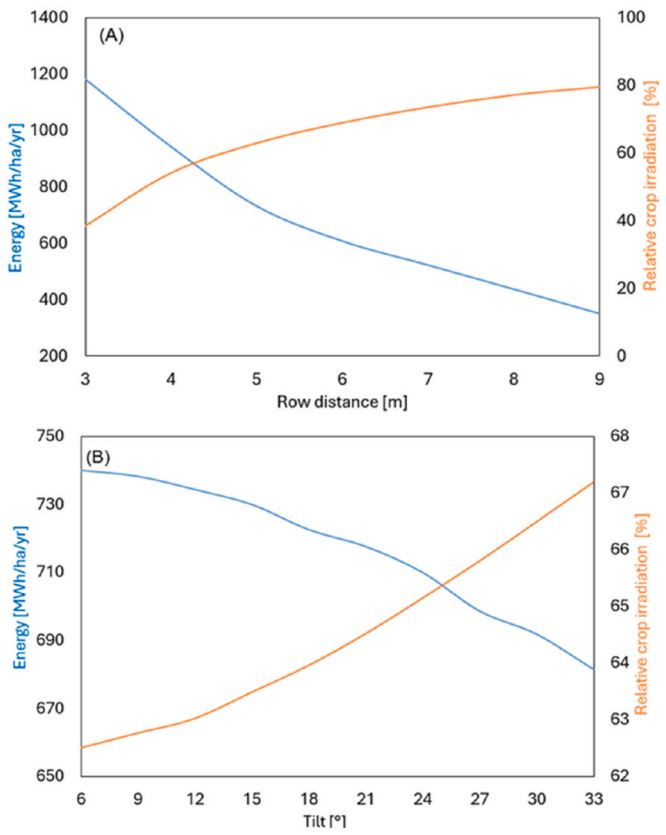

Fig. 11. Annual relative crop irradiation and energy yield for EW wing system for (A) varied row distances at 12° tilt and (B) varied tilt angles at 5 m row distance.

3.2. Assessing the crop irradiation

The average crop irradiance was assessed for a typical arable farming season in Belgium (March to October) as shown in Fig. 12. Rows of high solar irradiation were recorded in the regions closest to the PV arrays of the EW vertical system as indicated by the green arrows. These regions are relatively less shaded compared to central ground areas between PV arrays (also seen in Fig. 9), especially during the hours before and after solar noon when the shadows are more extended towards the central ground areas. In addition, these regions are less obstructed due to the elevation of the PV modules, hence, the higher irradiation rows observed. Generally, these areas under and closest to the PV rows in EW vertical systems are not used for crop cultivation, and as such no impact on crop yields is expected. Nevertheless, these areas could offer potential applications for other farming practices such as beekeeping for increased biodiversity and pollination in farming systems. High solar irradiation was also recorded in the central corridors between the vertical PV rows due to minimal shading around solar noon. The checkerboard and dash-line patterns reduced the heterogeneity of the crop irradiance while the irradiance between the PV rows also increased. However, the dash-line also created irradiation patches as indicated by the black arrows in Fig. 12C.

The EW wing system created the most homogeneous crop irradiance as shown in Fig. 12D–F. Arranging the PV panels in checkerboard and dash-line patterns had little effect on the homogeneity of the light distribution although the total crop irradiance was higher due to the lower PV density and PV shading. The S-tilted system created permanently shaded rows as indicated by the red arrows in Fig. 12G. It was also reported that S-tilted AV systems created persistent shading [47]. Hence, S-tilted AV systems could be suitable for intercropping practices wherein shade-intolerant crops are grown on the areas with higher irradiance between the PV rows and shade tolerant crops cultivated under those permanently shaded areas (red arrows). The checkerboard and dash-line patterns reduced this disparity in irradiance. Nevertheless, the heterogeneity created by the alternating shaded and unshaded rows was still discernible as seen in Fig. 12H–I.

Analysis of the crop irradiance distribution was supplemented with the total yearly crop irradiation for the different AV configurations as shown in Fig. 13. The EW vertical system provided the highest crop irradiation mainly due to minimal PV shading around solar noon when the solar intensity is highest (Fig. 14). Hence, such systems could be suitable for permanent or perennial crops, grasslands, and shade-intolerant plants. However, the low PV elevations in such AV systems limit the crop types that can be grown between the PV arrays, as tall crops would lead to PV shading and reduced energy yield. The EW wing system created the highest shading, making it suitable for shade tolerant or C3 crops such as rice, wheat, soybeans, and barley. The lower (half) PV density in both the checkerboard and dash-line patterns increased the total crop irradiation for all AV systems compared to straight-line pattern. The checkerboard and dash-line patterns both led to similar total crop irradiation and the gains in yearly crop irradiation for the checkerboard and dash-line patterns compared to the straight-line were 9.8% for the EW vertical, 29.4% for the EW wing and 28.1% for the S-tilted. Hence the dash-line and checkerboard patterns resulted in the lowest gain in the total crop irradiation for the EW vertical system. Due to the minimum crop shading around solar noon for the EW vertical (Fig. 14), this low gain in crop irradiation with lower PV density is expected. Therefore, the main benefit of such PV module patterns for the EW vertical system is an increase in the uniformity of the crop irradiance distribution as shown in Fig. 12B–C compared to the straight-line design

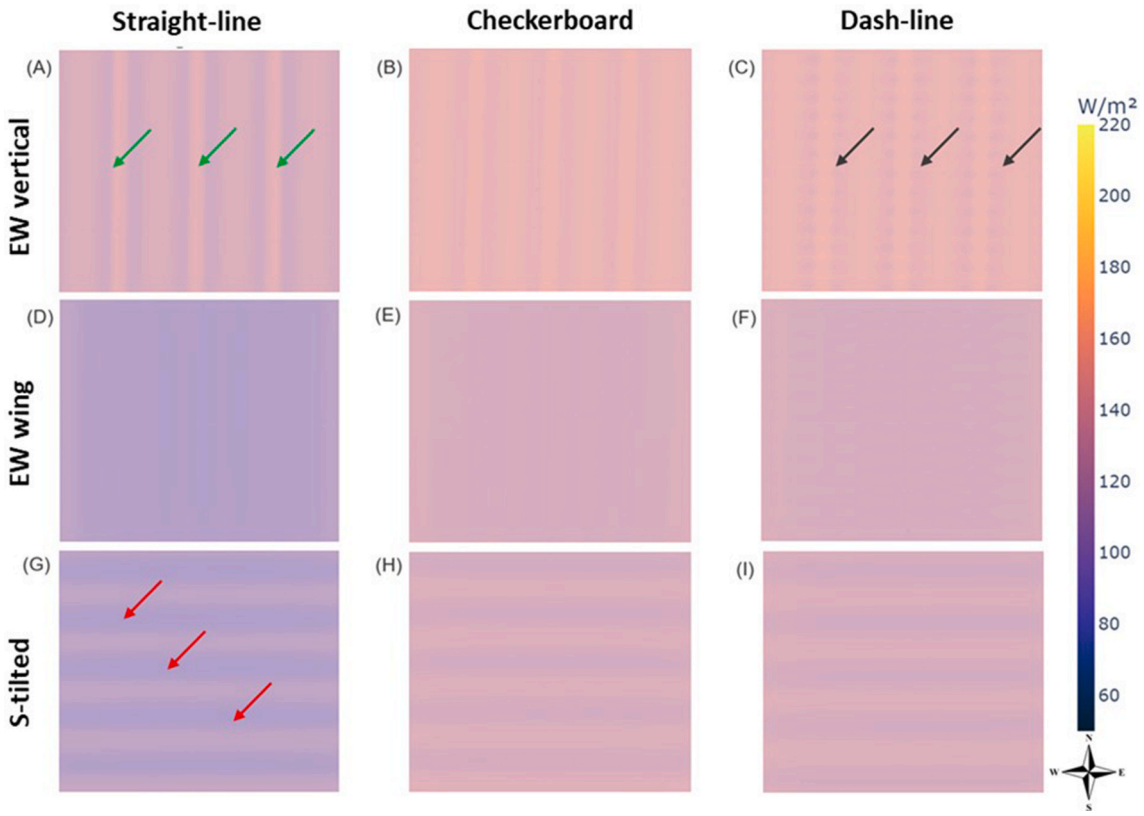

Fig. 12. Average crop irradiance distribution for the EW vertical, EW wing and S-tilted AV designs. Irradiance shown for a typical arable farming season (March–October).

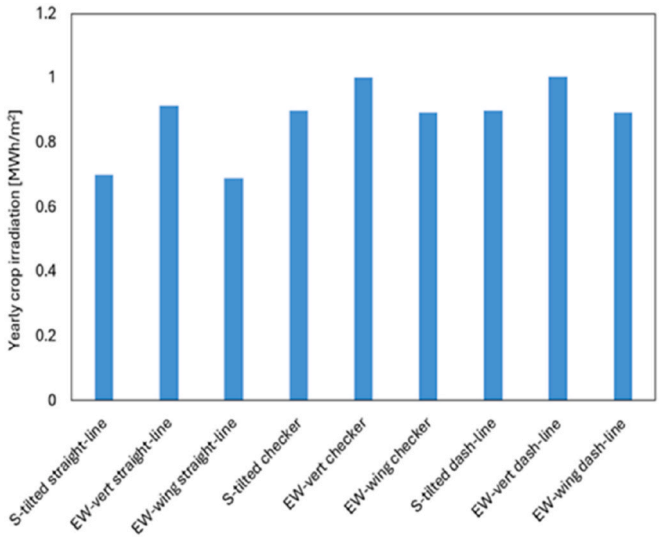

Fig. 13. Total yearly crop irradiation for the different AV topologies.

(Fig. 12A).

It should also be noted that due to the absence of the mounting and support structures in this study, the actual crop irradiation would be less than those reported in this work. The level of shading is expected to be lower for the interspace (EW vertical) system due to the lower height of the mounting structures compared to the overhead (S-tilted and EW wing) AV systems. Nevertheless, the land loss and subsequent reduction in crop yield and land productivity due to the support structures and related safety margins for operating agricultural machinery was considered as mentioned in section 2.5.

3.3. Power and energy yield

Knowledge of the power output profiles helps in determining grid-connectivity requirements and in choosing AV systems which meet different load profiles. Fig. 15 shows the power output profiles for the EW vertical, EW wing and S-tilted AV systems for a clear sky day in June. The EW vertical system had two power production peaks contrary to the S-tilted and EW wing systems which had one prominent peak around noon. Hence, EW vertical systems spread the power generation more uniformly and have a closer match with typical load profiles. This improves the self-consumption of PV production on the farm, thereby reducing grid congestion issues. The EW vertical power generation profile also prevents overproduction at midday and associated grid connectivity issues such as power curtailment. This shift in power generation could also reduce the need for energy storage systems due to better energy supply-demand balance [48]. This would reduce the need and costs for electrical storage equipment. In an energy system model for Germany in which 80% of the S-tilted PV systems were replaced by EW vertical systems without storage, it was reported that CO_2 emissions could be reduced by up to 10.2 Mt/a [49]. This was due to a better balance in energy demand-supply and hence reduced electricity demand from flexible fossil gas-fired power plants. The power generation profile of EW vertical systems also makes them suitable for areas with network bottlenecks [50].

The yearly energy yield for a capacity equivalent for the AV systems was also calculated as shown in Fig. 16. The S-tilted AV system produced the highest specific energy followed by the EW wing. For the straight-line patterns, the yearly specific energy yield for the S-tilted system was 1070 kWh/kW_p, which was 25% higher than the EW vertical and 19.3% higher than the EW wing system. Furthermore, the percentage difference in energy yield between the S-tilted and the EW wing and EW vertical systems was much higher in the winter periods compared to the summer as seen in Fig. 17. The maximum difference in energy yield

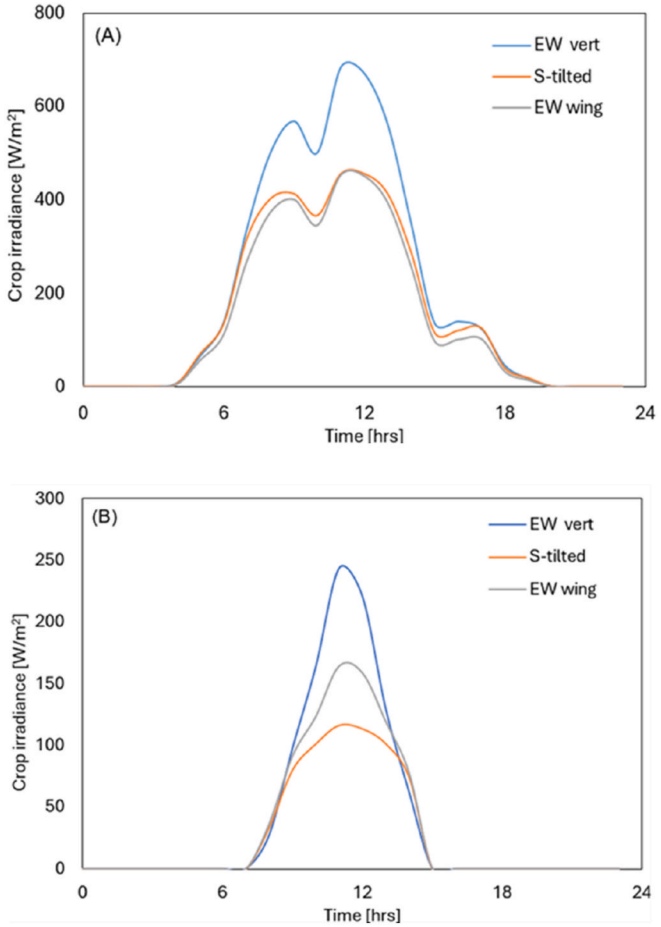

Fig. 14. Crop irradiance profiles for the AV systems (straight-line) on (A) summer solstice (June 21) and (B) winter solstice (December 21). Time in UTC.

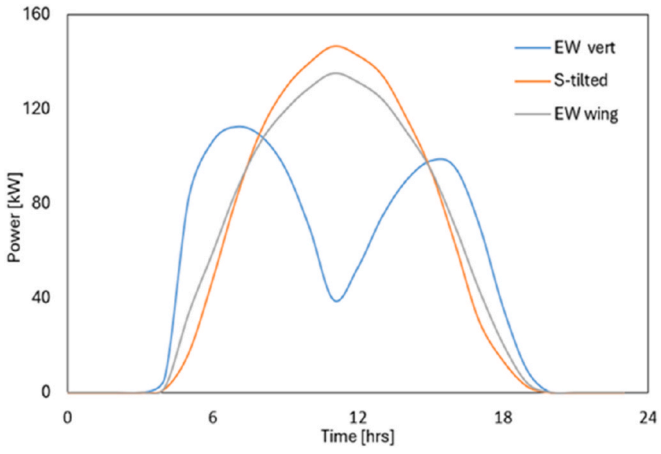

Fig. 15. Power output profiles of the EW wing, EW vertical and S-tilted AV systems on a clear sky day (June 25). Time in UTC.

between the S-tilted and EW vertical was 79.8% which was recorded in December, while a minimum of 10.6% was recorded in July. Similarly, the highest difference in energy yield between the S-tilted and EW wing was 103.6%, also recorded in December while only 0.4% gain was recorded in June. Hence, in the winter periods, the S-tilted system seems to amplify the energy yield compared to the EW vertical and EW wing systems.

For each AV configuration, the checkerboard and dash-line patterns

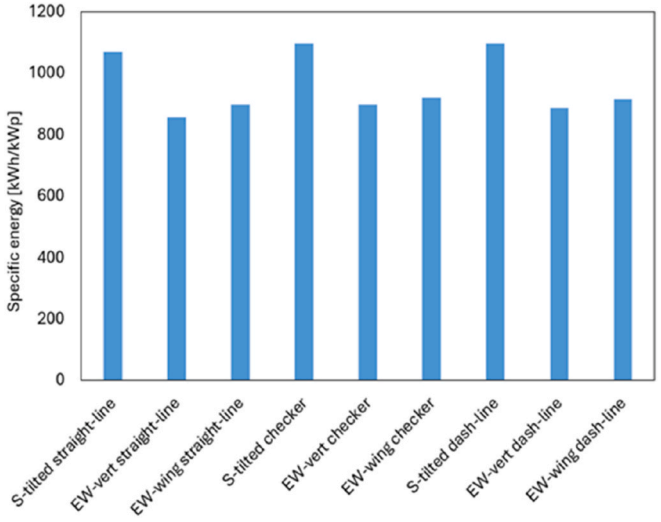

Fig. 16. Yearly specific energy yield for the different AV topologies.

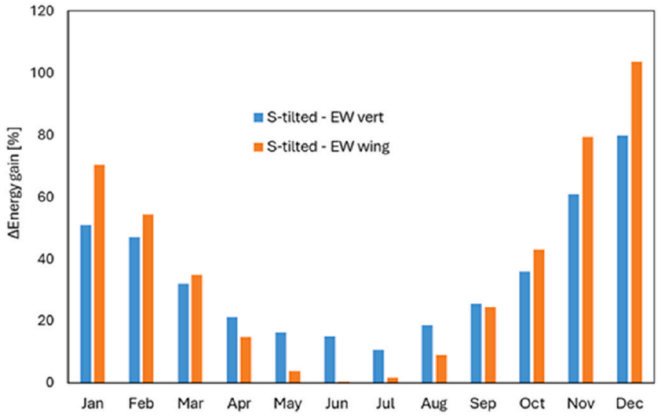

Fig. 17. Seasonal variations in energy gain for S-tilted compared to the EW vertical and EW wing systems.

both had comparable specific energy yields, which were respectively 1096.3 kWh/kW$_p$ and 1097 kWh/kW$_p$ for the S-tilted, 897 kWh/kW$_p$ and 887.7 kWh/kW$_p$ for the EW vertical and 919.4 kWh/kW$_p$ and 915.5 kWh/kW$_p$ for the EW wing system. The specific energy yields for the checkerboard and dash-line patterns were about 2.5%, 4.2% and 2.3% higher than the straight-line for the S-tilted, EW vertical and EW wing systems respectively. This was due to higher rear side PV irradiance, leading to a higher gain in bifacial energy. As the support structures were not considered, a further reduction in the reported energy yields could be expected. The presence of these structures is expected to reduce the rear side PV irradiance (reflected and diffuse) and hence the bifacial energy gain.

The specific energy yield is a suitable performance metric to compare the energy output for different PV systems. However, the land needed for the same installed capacity differs from one AV configuration to another. This is mainly due to the different PV design requirements such as the row distances, elevation, and the tilt angles. For example, in EW vertical systems, the PV modules are installed at higher row distances to avoid mutual PV shading and to provide sufficient passage for agricultural machinery while the overhead systems are installed at higher elevations to provide room for agricultural machinery and human activity. In addition, the PV density of the checkerboard and dash-line systems is half that of the straight-line (standard) design. Therefore, the overall performance of the different AV topologies was further assessed for the same land area. Fig. 18 summarizes these findings.

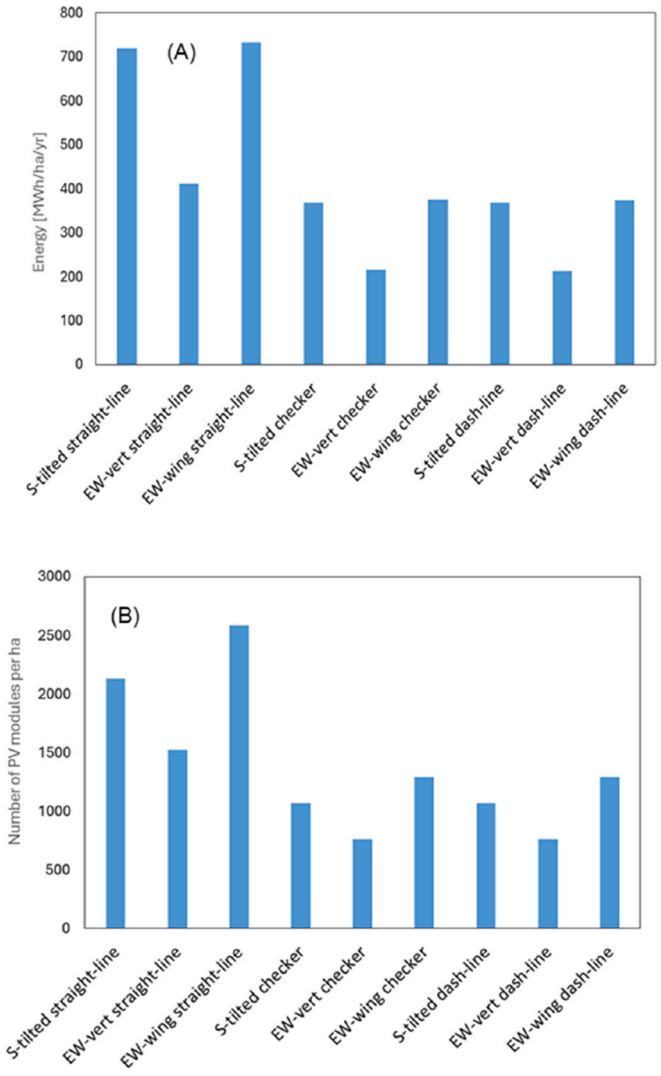

Fig. 18. Performance comparison of the different AV designs for same land area (1 ha), based on (A) energy yield (B) number of installed PV modules.

The EW wing system was less land intensive as it enabled about 21.4% and 70% higher PV installed capacity compared to the S-tilted and EW vertical respectively for 1 ha of land. This resulted in 1.8% and 78.1% gain in yearly energy yield compared to the S-tilted and EW vertical systems respectively. Coupled with the maximum shading and homogeneous irradiation distribution, EW wing systems could therefore offer the best combination of energy yield and crop protection, enabling the cultivation of shade tolerant and soft fruits (e.g., berries, grapes, black- and red currants) which could be susceptible to sunburn.

The EW vertical system had the lowest PV installed capacity mainly due to the higher row distances. However, the total irradiation reaching the crops was highest for the EW vertical system, allowing the cultivation of shade-intolerant or permanent crops. Nevertheless, due to minimal shading at solar noon (Fig. 14), crops in EW vertical systems could experience high temperatures and associated evapotranspiration which could potentially cause high water stress and potential stomata flaccidity [51]. Such conditions would reduce the CO_2 assimilation and the net photosynthesis rate [52].

3.4. Crop yields and LER for the simulated AV topologies

The simulated grain yields for winter wheat and root yield for sugar beets (in t DM/ha) under the AV (shaded) and the reference (open-field) conditions are presented in Fig. 19. These values are compared to values reported in literature to determine if the simulated yields across the different AV configurations are suitable for further analysis. For example, in an agroforestry (non-AV) study in Belgium, winter wheat yields of ~11–12 t DM/ha were reported [53], which is closely aligned with the output from this model in open-field conditions. However, the winter wheat yields from the open and AV systems in this work are higher than those (4.6 t/ha for the control) reported in Ref. [54]. This discrepancy may be due to factors such as specific weather conditions, agricultural practices, and model input parameters (e.g., radiation use efficiency, max LAI). These factors suggest that further calibration of key input parameters to the specific conditions of those studies may be needed for greater accuracy. For sugar beets, the model predicted an open-field yield of 20.61 t DM/ha, which is consistent with previous studies where yields of ~20–22 t DM/ha were reported for sugar beets under no shade conditions in Belgium [55]. The open field results are also comparable to that (~22–27 t DM/ha) previously reported in Ref. [53]. Furthermore, yields between 18.2 and 22.6 t DM/ha are expected (in 2024) for different sugar beet varieties grown in Belgium [56]. Therefore, the simulated crop yields from the given inputs appear comparable, supporting their use for further analysis in this study.

The yields of both winter wheat and sugar beet were highest under the EW vertical system followed by the S-tilted system. The higher yields are attributed to the higher solar irradiation reaching the crops. The crop yields were also higher under the lower PV densities, (dash-line and checkerboard), compared to the standard density. Up to 31% increase in winter wheat and sugar beet yields was observed under both the EW wing checkerboard and dash-line configurations compared to the standard EW wing layout. Given the uniform light distribution in the EW wing system, crops in such systems will also benefit from uniform growth and fruit ripening. The lowest increase in crop yield (9.7%) with lower PV density was recorded for sugar beet in the EW vertical system. This was mainly attributed to the low gain in crop irradiation with lower PV density compared to the EW wing and S-tilted designs. For sugar beet, root dry matter has been shown to increase with solar irradiation and is independent of morphological adaptations under shade [55]. Sugar beet yield reduction under an AV set up was also reported in Ref. [54], and sugar beet yields are expected to reduce in either yield or quality (sugar level) or both under continuous shade [57].

For winter wheat, differences in yield under different shading scenarios have been reported. Past trials with winter wheat have shown that relatively low intensity shading (up to 15%) improved the yield of winter wheat variety Yangmai 158 [58]. This was attributed to plant

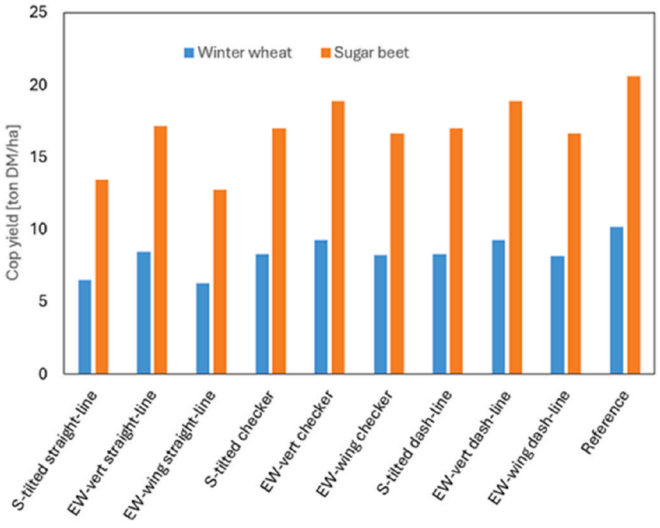

Fig. 19. Yields of winter wheat and sugar beet under AV systems and the reference (full sun).

adaptation including increased LAI, enlarged and thin upper leaves, increased peduncle internode length, increased pigment content, and enhanced redistribution of dry matter into grains [58]. However, cultivar Yangmai 11 (shade sensitive) showed lower yields under similar shading conditions [58]. Differences in grain yield for various winter wheat cultivars under shading conditions in North China Plain were also reported [59]. Furthermore, harvestable yields of winter wheat under an AV set up in Germany reduced by 19% in 2017 and increased by 3% in 2018 (dry and hot summer) [60]. AV systems could therefore mitigate the effects of drought on winter wheat yields [61]. Hence, the yield of winter wheat is also highly dependent on the cultivar, climate, and the location.

From the crop and energy yields, the calculated LERs are shown in Fig. 20. Table S6 in Supporting Information summarizes the energy and crop yields used in calculating the LER for the different AV systems. The electrical energy yield for the GMPV system defined in section 2.5 was 1181.6 MWh/ha/yr. For both winter wheat and sugar beet, highest LERs of 1.18 and 1.20 respectively were recorded under the S-tilted system, while the lowest LER of 1.0 was obtained for the EW vertical half PV density designs. Given the higher crop yields under the EW vertical systems compared to the S-tilted and EW wing, the lower LER was due to the lower energy yield (as seen in Table S6 in Supporting Information). A similar LER was obtained in 2021 for sugar beets grown under an EW vertical pilot site in Grembergen (Belgium) [54]. For both winter wheat and sugar beets, the LER ratio was also lower for the half PV density systems compared to the standard density, mainly due to the lower PV energy yield. Hence, for crops which have been shown to adapt under shading conditions, lower PV densities might not be desired as the total energy yield is reduced resulting in lower total land productivity. Nevertheless, the increased crop yield and enhanced crop light distribution resulting from the half PV density designs is desired for agricultural profitability. For each AV orientation, the LERs for the dash-line and checkerboard designs were comparable. Furthermore, for both winter wheat and sugar beet, the LER ratio for the straight-line patterns was 13.2%, 9.3% and 12.6% higher than that of the half-PV density designs for the S-tilted, EW vertical and EW wing systems respectively. For all AV topologies presented in this study, the land use efficiency was enhanced for both winter wheat and sugar beet.

4. Limitations of this study and outlook

In this work, a yearly soiling loss of 5% was considered in the PV energy yield. However, there could be some variations in the soiling rate due to the tilt angles and orientations of the studied AV systems [62].

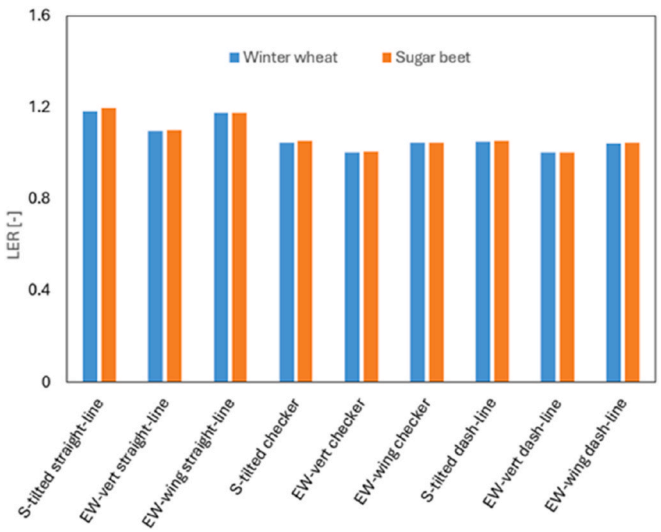

Fig. 20. LERs for winter wheat and sugar beet under the different AV systems.

Power losses due to soiling could be reduced by implementing and combining PV cleaning with irrigation systems, which could be very beneficial in drylands [63]. In addition, seasonal variations in soiling levels need to be accounted for to better assess the soiling losses.

In the irradiance modelling, the shading impact of the mounting structures was neglected in this work. Due to the differences in elevation for overhead and interspace systems, the shading losses from the support structures will be different. These additional shading losses could potentially reduce the crop irradiation, and the crop and energy yields reported. Accurate modelling of these structures is needed and ongoing to correctly predict their shading effects on the crops. Furthermore, while the checkerboard and dash-line designs enhanced the crop irradiation and crop yields compared to the straight-line, the capital expenditure for such AV designs is expected to be higher. This is because the engineering process (planning, preparation, installation) and costs (mounting structures and wiring) of such AV systems are respectively more complex and higher. Research on the economic performance of the different designs is beyond the scope of this work.

Another limitation in this study is in the crop model. It was assumed that the crop-specific input parameters (Table S4) remained consistent throughout the growing period for all the AV systems. This means that crop adaptation to prolonged shading under the studied AV designs was not included, hence no calibration of the crop-specific input parameters was applied. In reality, the PAR intercepted by crops is dependent on the crop canopy structure defined by the LAI, which changes during crop development. Under prolonged shading conditions, crops have been shown to adapt by developing different morphological and physiological traits such as an increase in their total leaf area [19,58] to intercept more light. Therefore, the crop yields presented in this study could be lower than actual values in AV systems. Nevertheless, the impact of reduced solar irradiation (i.e., reduced PAR) and subsequent effects on other microclimatic parameters (e.g., lower surface temperatures due to the PV shading) on the crops have been represented.

Given the lower PV density in AV systems compared to GMPV, the total energy yield is expected to be lower. To increase the specific energy yield, there is a continuous growth in the installation of bifacial PV modules. As the PV modules in AV systems are installed at higher elevations and row distances compared to GMPV systems, the amount and uniformity of the rear PV irradiance is enhanced resulting in higher bifacial gain. A further boost in bifacial energy gain lies in the use of albedo boosters [64]. Certain farming practices such as orchard farming could offer rows of unused land between the crops for the implementation of albedo boosters. These boosters could also be fully implemented during non-farming periods (off-seasons) in farming practices where the land underneath the PV modules is not being used. Moreover, the specific energy yield would be further enhanced in the lower PV density designs due to the higher ground irradiation and bifacial gain. However, efficient cleaning regimes must be implemented to maintain the performance of the albedo boosters, while soiling and degradation models must consider their soiling rates for accurate PV energy yield predictions.

5. Conclusions

In AV systems, light can be the main limiting resource, especially for crops with high light requirements. Therefore, AV configurations which enhance light sharing between PV panels and crops need to be studied and implemented. In this study, a modelling approach which integrates irradiance modelling with PV energy and crop yield modelling was used to assess the performance of nine different bifacial AV topologies: S-tilted, EW vertical and EW wing AV systems each arranged in straight-line (standard), checkerboard and dash-line patterns. Using winter wheat and sugar beets for the location of Genk, Belgium (temperate climate) as a case study, the crop and energy yields and the total land productivity for each AV topology were assessed.

In AV systems, edge effect minimization is required to faithfully

identify the underlying design parameters which impact the energy yield and shading on crops. AV test sites for validation must also meet the minimal farm size for which edge effects are minimized. We proposed for the climate studied a minimum ground area of 0.26 ha, for which the selected central AV area should be approximately 0.02 ha.

For the AV configurations studied, the S-tilted system had the highest specific energy yield of 1070 kWh/kW_p, which was 25% higher than the EW vertical and 19.3% higher than the EW wing system. The S-tilted system also amplified the energy yield in the winter months compared to EW vertical and EW wing systems. Furthermore, the specific energy yield was enhanced under the half density checkerboard and dash-line designs compared to the standard layout, with the highest increase of 4.2% for the EW vertical.

EW vertical systems created the highest crop irradiation and resulted in higher crop yields compared to EW wing and S-tilted systems. The S-tilted AV system created permanent shading patterns while the checkerboard and dash-line arrangements increased the homogeneity. The standard EW wing system offered the best crop protection, and the most homogeneous crop light distribution. However, the crop irradiation and crop yields were lowest.

Crop yields were enhanced under the lower PV densities due to enhanced crop irradiation, with up to 31% increase in winter wheat and sugar beet yields under EW wing checkerboard and dash-line compared to the EW wing standard design. For all AV systems studied, the land productivity was enhanced for both crops, with the highest LER of 1.2 obtained for sugar beets under S-tilted straight-line design. For each AV orientation, the checkerboard and dash-line patterns both had similar land productivities.

Therefore, in regions with temperate climates, EW vertical systems could be suitable for enhancing crop yields compared to its S-tilted and EW wing counterparts. In addition, lower PV density designs such as the checkerboard and dash-line could help achieve higher and more uniform crop irradiation and increased crop yields. However, due to the fact that EW vertical systems are land intensive compared to the S-tilted and EW wing, the energy yield is much lower leading to a lower LER compared to the EW wing and S-tilted systems. Hence, as EW vertical systems showed the lowest gain in crop irradiation with reduced PV density compared to S-tilted and EW wing, a lower PV density might not be desired if land productivity is to be further enhanced. In addition, for crops such as winter wheat which have shown to adapt under shade (through enlarged and thin upper leaves to capture more light), the lower PV densities might not be required because the land productivity is reduced due to lower total energy yield.

Nevertheless, for all the AV topologies developed in this work, the total land productivity was enhanced, justifying the need for new AV topologies to help achieve some of the sustainable development goals and reduce the land use competition between PV and agriculture. This could be very valuable for regions with limited solar irradiation, high population densities and fragmented landscapes, looking to move towards AV systems.

CRediT authorship contribution statement

Shu-Ngwa Asa'a: Writing – review & editing, Writing – original draft, Visualization, Software, Methodology, Investigation, Formal analysis, Data curation, Conceptualization. **Silvia Ma Lu:** Writing – review & editing, Writing – original draft, Software, Methodology, Investigation, Formal analysis, Data curation. **Ismail Kaaya:** Writing – review & editing, Methodology, Formal analysis. **Olivier Dupon:** Writing – review & editing, Visualization, Software. **Richard de Jong:** Writing – review & editing, Software, Methodology. **Arvid van der Heide:** Writing – review & editing, Supervision. **Sara Bouguerra:** Writing – review & editing. **Hariharsudan Sivaramakrishnan Radhakrishnan:** Writing – review & editing, Supervision, Funding acquisition. **Jef Poortmans:** Writing – review & editing, Supervision. **Pietro Elia Campana:** Writing – review & editing, Supervision, Software, Funding acquisition. **Michael Daenen:** Writing – review & editing, Supervision.

Data availability

Data is available on request.

Funding

This work is funded by the European Union through the Horizon Europe Research and Innovation programme SYMBIOSYST under grant agreement no. 101096352 and the Fonds Wetenschappelijk Onderzoek (FWO) through the SB PhD Fellowship under grant number 1SHF024N. Financial support was also received from the Swedish Energy Agency through the project "The Solar Electricity Research Centre (SOLVE)", grant number 52693–1. The funders had no role in the study design, data collection, analysis, decision to publish, or preparation of this work.

Declaration of competing interest

The authors declare that they have no known competing financial interests or personal relationships that could have appeared to influence the work reported in this paper.

Acknowledgements

The authors would like to thank Alex Dewalque from the Royal Meteorological Institute (RMI) of Belgium for the precipitation data. The authors would also like to thank the reviewers for their time and the valuable feedback.

Appendix A. Supplementary data

Supplementary data to this article can be found online at https://doi.org/10.1016/j.renene.2025.123528.

References

[1] Going climate-neutral by 2050 - Publications office of the EU." Accessed: February. 14, 2025. [Online]. Available: https://op.europa.eu/en/publication-detail/-/publication/92f6d5bc-76bc-11e9-9f05-01aa75ed71a1.
[2] Snapshot of global PV markets 2025 task 1 strategic PV analysis and outreach PVPS", Accessed: April. 25, 2025. [Online]. Available: https://iea-pvps.org/wp-content/uploads/2025/04/Snapshot-of-Global-PV-Markets_2025.pdf.
[3] Population | united nations." Accessed: February. 16, 2024. [Online]. Available: https://www.un.org/en/global-issues/population.
[4] Landscape fragmentation pressure in Europe | european environment Agency's home page." Accessed: February. 14, 2025. [Online]. Available: https://www.eea.europa.eu/en/analysis/indicators/landscape-fragmentation-pressure-in-europe.
[5] S. Asa'a, et al., A multidisciplinary view on agrivoltaics: future of energy and agriculture, Renew. Sustain. Energy Rev. 200 (Aug. 2024) 114515, https://doi.org/10.1016/J.RSER.2024.114515.
[6] M.A. Al Mamun, P. Dargusch, D. Wadley, N.A. Zulkarnain, A.A. Aziz, A Review of Research on Agrivoltaic Systems, Elsevier Ltd, Jun. 01, 2022, https://doi.org/10.1016/j.rser.2022.112351.
[7] M. Trommsdorff et al., "Agrivoltaics: opportunities for agri-culture and the energy transition", Accessed: April. 27, 2023. [Online]. Available: https://www.ise.fraunhofer.de/content/dam/ise/en/documents/publications/studies/APV-Guideline.pdf.
[8] Population density | statbel." Accessed: February. 16, 2024. [Online]. Available: https://statbel.fgov.be/en/themes/population/structure-population/population-density.
[9] A. Verhoeve, V. Dewaelheyns, E. Kerselaers, E. Rogge, H. Gulinck, Virtual farmland: grasping the occupation of agricultural land by non-agricultural land uses, Land Use Policy 42 (Jan. 2015) 547–556, https://doi.org/10.1016/J.LANDUSEPOL.2014.09.008.
[10] Pears under solar panels | KU leuven stories [Online]. Available: https://stories.kuleuven.be/en/stories/pears-under-solar-panels. (Accessed 6 May 2025).
[11] Electricity mix for Belgium in 2024: record international exchanges, significant increase in solar generation, and low use of gas-fired capacities." Accessed: January. 29, 2025. [Online]. Available: https://www.elia.be/en/press/2025/01/20250102_electricity-mix.
[12] Belgium climate resilience policy indicator – analysis - IEA." Accessed: May 6, 2025. [Online]. Available: https://www.iea.org/reports/belgium-climate-resilience-policy-indicator.

[13] Belgium (flanders) - european commission." Accessed: July. 22, 2024. [Online]. Available: https://agriculture.ec.europa.eu/cap-my-country/cap-strategic-plans/belgium-flanders_en.
[14] H.J. Williams, K. Hashad, H. Wang, K. Max Zhang, The potential for agrivoltaics to enhance solar farm cooling, Appl. Energy 332 (Feb. 2023) 120478, https://doi.org/10.1016/j.apenergy.2022.120478.
[15] B. Willockx, et al., How agrivoltaics can be used as a crop protection system, in: EUROSIS Proceedings, 2022, pp. 130–136.
[16] H. Marrou, L. Dufour, J. Wery, How does a shelter of solar panels influence water flows in a soil–crop system? Eur. J. Agron. 50 (Oct. 2013) 38–51, https://doi.org/10.1016/J.EJA.2013.05.004.
[17] H. Dinesh, J.M. Pearce, The Potential of Agrivoltaic Systems, Elsevier Ltd., Feb. 01, 2016, https://doi.org/10.1016/j.rser.2015.10.024.
[18] A. Weselek, A. Ehmann, S. Zikeli, I. Lewandowski, S. Schindele, P. Högy, Agrophotovoltaic systems: applications, challenges, and opportunities. A Review, Springer-Verlag France, Aug. 01, 2019, https://doi.org/10.1007/s13593-019-0581-3.
[19] H. Marrou, J. Wery, L. Dufour, C. Dupraz, Productivity and radiation use efficiency of lettuces grown in the partial shade of photovoltaic panels, Eur. J. Agron. 44 (Jan. 2013) 54–66, https://doi.org/10.1016/j.eja.2012.08.003.
[20] K. Ali Khan Niazi, M. Victoria, Comparative analysis of photovoltaic configurations for agrivoltaic systems in Europe, Prog. Photovoltaics Res. Appl. 31 (11) (Nov. 2023) 1101–1113, https://doi.org/10.1002/pip.3727.
[21] M.H. Riaz, H. Imran, R. Younas, N.Z. Butt, The optimization of vertical bifacial photovoltaic farms for efficient agrivoltaic systems, Sol. Energy 230 (Dec. 2021) 1004–1012, https://doi.org/10.1016/j.solener.2021.10.051.
[22] S. Lee, et al., Agrivoltaic system designing for sustainability and smart farming: agronomic aspects and design criteria with safety assessment, Appl. Energy 341 (Jul. 2023) 121130, https://doi.org/10.1016/J.APENERGY.2023.121130.
[23] B. Willockx, T. Reher, C. Lavaert, B. Herteleer, B. Van de Poel, J. Cappelle, Design and evaluation of an agrivoltaic system for a pear orchard, Appl. Energy 353 (Jan) (2024), https://doi.org/10.1016/j.apenergy.2023.122166.
[24] O.A. Katsikogiannis, H. Ziar, O. Isabella, Integration of bifacial photovoltaics in agrivoltaic systems: a synergistic design approach, Appl. Energy 309 (Mar) (2022), https://doi.org/10.1016/j.apenergy.2021.118475.
[25] I.T. Horváth, et al., Photovoltaic energy yield modelling under desert and moderate climates: what-If exploration of different cell technologies, Sol. Energy 173 (Oct. 2018) 728–739, https://doi.org/10.1016/j.solener.2018.07.079.
[26] H. Goverde, et al., Energy yield prediction model for PV modules including spatial and temporal effects, in: 29th European Photovoltaic Solar Energy Conference and Exhibition, 2014, pp. 3292–3296. ISBN: 3-936338-34-5. [Online]. Available: https://imec-publications.be/handle/20.500.12860/23873. (Accessed 21 February 2024).
[27] JRC photovoltaic geographical information system (PVGIS) - european commission." Accessed: November. 6, 2024. [Online]. Available: https://re.jrc.ec.europa.eu/pvg_tools/de/#TMY.
[28] D. Berrian, J. Libal, A comparison of ray tracing and view factor simulations of locally resolved rear irradiance with the experimental values, Prog. Photovoltaics Res. Appl. 28 (6) (Jun. 2020) 609–620, https://doi.org/10.1002/PIP.3261.
[29] RADIANCE detailed description — Radsite." Accessed: February. 21, 2024. [Online]. Available: https://www.radiance-online.org/archived/radsite/radiance/refer/long.html.
[30] R. Perez, R. Seals, P. Ineichen, R. Stewart, D. Menicucci, A new simplified version of the perez diffuse irradiance model for tilted surfaces, Sol. Energy 39 (3) (Jan. 1987) 221–231, https://doi.org/10.1016/S0038-092X(87)80031-2.
[31] O. Virtanen, E. Constantinidou, E. Tyystjärvi, Chlorophyll does not reflect green light–how to correct a misconception, J. Biol. Educ. 56 (5) (2022) 552–559, https://doi.org/10.1080/00219266.2020.1858930.
[32] G. Ward Larson, Rob Shakespeare, Charles Ehrlich, John Mardaljevic, Erich Phillips, Peter Apian-Bennewitz, Rendering with Radiance : the Art and Science of Lighting Visualization, 1998, p. 664.
[33] Shravan K. Chunduri, Michael Schmela, Bifacial solar module technology 2018 edition - getting ready for much higher yields with bifacial modules. https://doi.org/10.13140/RG.2.2.11521.17765, Jun. 2018.
[34] Q. Zhu, et al., A model to evaluate the effect of shading objects on the energy yield gain of bifacial modules, Sol. Energy 179 (Feb. 2019) 24–29, https://doi.org/10.1016/J.SOLENER.2018.12.006.
[35] P.E. Campana, B. Stridh, S. Amaducci, M. Colauzzi, Optimisation of vertically mounted agrivoltaic systems, J. Clean. Prod. 325 (Nov) (2021), https://doi.org/10.1016/j.jclepro.2021.129091.
[36] J.R. Williams, C.A. Jones, J.R. Kiniry, D.A. Spanel, The EPIC crop growth model, Trans. ASAE (Am. Soc. Agric. Eng.) 32 (2) (1989) 497–511.
[37] Agricultural production - crops - statistics explained." Accessed: February. 17, 2025. [Online]. Available: https://ec.europa.eu/eurostat/statistics-explained/index.php?title=Agricultural_production_-_crops.
[38] A. Gobin, Modelling climate impacts on crop yields in Belgium, Clim. Res. 44 (1) (2010) 55–68, https://doi.org/10.3354/CR00925.
[39] Weather in Belgium - IRM." Accessed: November. 6, 2024. [Online]. Available: https://www.meteo.be/fr/belgique.
[40] M.G. dos Reis, A. Ribeiro, Conversion factors and general equations applied in agricultural and forest meteorology, Agrometeoros 27 (2) (Mar. 2020), https://doi.org/10.31062/AGROM.V27I2.26527.
[41] C. Dupraz, H. Marrou, G. Talbot, L. Dufour, A. Nogier, Y. Ferard, Combining solar photovoltaic panels and food crops for optimising land use: towards new agrivoltaic schemes, Renew. Energy 36 (10) (Oct. 2011) 2725–2732, https://doi.org/10.1016/j.renene.2011.03.005.
[42] Ray tracing | NVIDIA developer." Accessed: February. 20, 2023. [Online]. Available: https://developer.nvidia.com/discover/ray-tracing.
[43] M. Prilliman, et al., Technoeconomic analysis of changing PV array convective cooling through changing array spacing, IEEE J Photovolt 12 (6) (Nov. 2022) 1586–1592, https://doi.org/10.1109/JPHOTOV.2022.3201464.
[44] K.R. Mcintosh, et al., Irradiance on the upper and lower modules of a two-high bifacial tracking system, in: PREPRINT FOR 47th IEEE PVSC, 2020.
[45] J. Guerrero-Perez and S. Chaouki-Almagro, "Bifacial trackers, the real deal. Bifacial gain and production analysis at BiTEC," Soltec Report. Accessed: February. 26, 2024. [Online]. Available: https://www.energias-renovables.com/ficheroenergias/documentos/White-Paper-BiTEC-Results-Bifacial-Trackers-the-Real-Deal.pdf.
[46] N. Hussain, et al., Study of soiling on PV module performance under different environmental parameters using an indoor soiling station, Sustain. Energy Technol. Assessments 52 (Aug. 2022) 102260, https://doi.org/10.1016/J.SETA.2022.102260.
[47] T. Obergfell, et al., Combining PV and Food Crops to Agrophotovoltaic ? Optimization of Orientation and Harvest, 2012, https://doi.org/10.4229/27thEUPVSEC2012-5AV.2.25.
[48] S. Obara, D. Konno, Y. Utsugi, J. Morel, Analysis of output power and capacity reduction in electrical storage facilities by peak shift control of PV system with bifacial modules, Appl. Energy 128 (Sep. 2014) 35–48, https://doi.org/10.1016/J.APENERGY.2014.04.053.
[49] S. Reker, J. Schneider, C. Gerhards, Integration of vertical solar power plants into a future German energy system, Smart Energy 7 (Aug. 2022) 100083, https://doi.org/10.1016/J.SEGY.2022.100083.
[50] C. Meyer, Agro PV – next2Sun's vertical installations, in: 6th Bifi PV Workshop, 2019.
[51] P. Jalakas, Y. Takahashi, R. Waadt, J.I. Schroeder, E. Merilo, Molecular mechanisms of stomatal closure in response to rising vapor pressure deficit, New Phytol. 232 (2) (Oct. 2021) 468, https://doi.org/10.1111/NPH.17592.
[52] H. Pirasteh-Anosheh, A. Saed-Moucheshi, H. Pakniyat, M. Pessarakli, Stomatal responses to drought stress, Water Stress and Crop Plants: A Sustainable Approach 1–2 (Jan. 2016) 24–40, https://doi.org/10.1002/9781119054450.CH3.
[53] P. Pardon, et al., Juglans regia (Walnut) in temperate arable agroforestry systems: effects on soil characteristics, arthropod diversity and crop yield, Renew. Agric. Food Syst. 35 (5) (Oct. 2020) 533–549, https://doi.org/10.1017/S1742170519000176.
[54] T. Reher, et al., Potential of sugar beet (beta vulgaris) and wheat (Triticum aestivum) production in vertical bifacial, tracked, or elevated agrivoltaic systems in Belgium, Appl. Energy 359 (Apr) (2024), https://doi.org/10.1016/j.apenergy.2024.122679.
[55] S. Artru, L. Lassois, F. Vancutsem, B. Reubens, S. Garré, Sugar beet development under dynamic shade environments in temperate conditions, Eur. J. Agron. 97 (Jul. 2018) 38–47, https://doi.org/10.1016/J.EJA.2018.04.011.
[56] Fodder beets - ILVO vlaanderen." Accessed: November. 6, 2024. [Online]. Available: https://rassenlijst.ilvo.vlaanderen.be/en/list-per-crop/fodder-beets.
[57] D.J. Watson, T. MOTOMATSU, K. LOACH, G.F.J. MILFORD, Effects of shading and of seasonal differences in weather on the growth, sugar content and sugar yield of sugar-beet crops, Ann. Appl. Biol. 71 (2) (Jul. 1972) 159–185, https://doi.org/10.1111/J.1744-7348.1972.TB02950.X.
[58] H. Li, D. Jiang, B. Wollenweber, T. Dai, W. Cao, Effects of shading on morphology, physiology and grain yield of winter wheat, Eur. J. Agron. 33 (4) (Nov. 2010) 267–275, https://doi.org/10.1016/J.EJA.2010.07.002.
[59] B. Dong, et al., Effects of shading stress on grain number, yield, and photosynthesis during early reproductive growth in wheat, Crop Sci. 59 (1) (Jan. 2019) 363–378, https://doi.org/10.2135/CROPSCI2018.06.0396.
[60] M. Trommsdorff, et al., Combining food and energy production: design of an agrivoltaic system applied in arable and vegetable farming in Germany, Renew. Sustain. Energy Rev. 140 (Apr. 2021) 110694, https://doi.org/10.1016/J.RSER.2020.110694.
[61] L. Pataczek, et al., Agrivoltaics mitigate drought effects in winter wheat, Physiol Plant 175 (6) (Nov. 2023) e14081, https://doi.org/10.1111/PPL.14081.
[62] S. Ali Sadat, J. Faraji, M. Nazififard, A. Ketabi, The experimental analysis of dust deposition effect on solar photovoltaic panels in Iran's desert environment, Sustain. Energy Technol. Assessments 47 (Oct. 2021) 101542, https://doi.org/10.1016/J.SETA.2021.101542.
[63] S. Ravi, et al., Colocation opportunities for large solar infrastructures and agriculture in drylands, Appl. Energy 165 (Mar. 2016) 383–392, https://doi.org/10.1016/J.APENERGY.2015.12.078.
[64] M.R. Lewis, S. Ovaitt, B. McDanold, C. Deline, K. Hinzer, Artificial ground reflector size and position effects on energy yield and economics of single-axis-tracked bifacial photovoltaics, Prog. Photovoltaics Res. Appl. (Oct. 2024), https://doi.org/10.1002/pip.3811.